

Effect of ultrasonic energy on nanoscale interfacial structure in copper wire bonding on aluminium pads

H Xu^{1,2}, C Liu², V V Silberschmidt², Z Chen³ and V L Acoff¹

¹ Department of Metallurgical and Materials Engineering, The University of Alabama, Tuscaloosa, Alabama 35487, USA

² Wolfson School of Mechanical and Manufacturing Engineering, Loughborough University, Loughborough, LE11 3TU, UK

³ School of Materials Science and Engineering, Nanyang Technological University, 50 Nanyang Avenue, Singapore 639798, Singapore

E-mail: HXu14@bama.ua.edu and huixu.hit@gmail.com

Received 12 October 2010, in final form 18 January 2011

Published 22 March 2011

Online at stacks.iop.org/JPhysD/44/145301

Abstract

The effect of ultrasonic vibration on nanoscale interfacial structure of thermosonic copper wire bonding on aluminium pads was investigated. It was found that bonding strength was determined by the extent of fragmentation of a native aluminium oxide overlayer (5–10 nm thick) on aluminium pads, forming paths for formation of intermetallic compound CuAl₂ in areas of direct contact of bonded metal surfaces. The degree of fracture of the oxide layer was strongly affected by a level of ultrasonic power.

1. Introduction

Wire bonding is the primary method of making electrical interconnections between the integrated circuits (ICs) and external circuitry in semiconductor packages. As compared with other chip interconnection methods including flip chip and tape automated bonding, it is the most cost-effective and flexible interconnect technology. Gold wires have been extensively used in wire bonding for tens of years, and recently, wire bonding using copper wire is becoming a preferred material due to its low cost, superior electrical, mechanical and thermal properties, and possible better reliability. In this process, a copper ball at the end of a wire is attached to an aluminium pad using a combination of ultrasonic energy, pressure (~150 MPa) and heat (150 °C–220 °C). It is a complex process, and the physics behind it has not been fully understood. Many attempts have been made to investigate and explain the process. In general, three experimental approaches have been employed to study the mechanisms of the bond formation. The first one concentrates on experimentally *in situ* measurements of interfacial temperature during bonding using specially designed sensors [1–5]. The second one considers an explanation of characteristics of the observed footprints on the bond pads or the bottom of the mashed

ball [6–10]. The third one is based on the cross-sectional characterization of the interfacial microstructure of bonds [11–14]. The main proposed theories include melting [15], fretting [16] and micro-slip [6, 17–19]. All those mechanisms assume that fracture of a ubiquitous native aluminium oxide overlayer is essential for successful bonding as it acts as a barrier to diffusion; this is verified experimentally by this work. Furthermore, although the effect of ultrasonic power on bonding strength was well documented [7, 20, 21], a full account of the underlying mechanistic aspects has not been presented. This is because that there were few reports on interfacial structural changes due to variation of ultrasonic power. Therefore, this study was undertaken to examine the effect of ultrasonic energy on interfacial characteristics of bonds, including degree of fracture of the aluminium oxide layer and formation of intermetallic compounds (IMCs). This approach leads to a relationship between ultrasonic power, interfacial structure and bonding strength.

2. Experimental

In the experiments, a copper wire (99.99 wt%/20 μm diameter) was bonded onto an aluminium pad on a silicon chip using

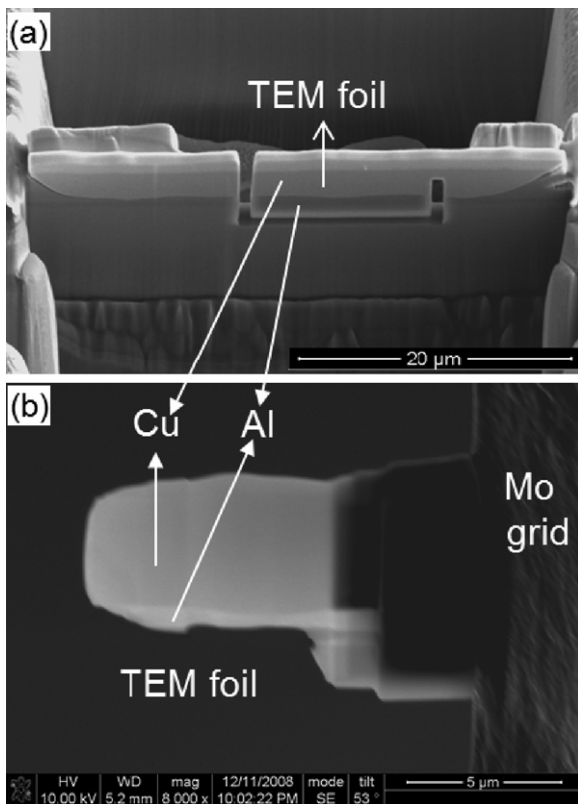


Figure 1. Region-specific TEM sample preparation with FIB: (a) TEM sample selected in the central area of bonds; (b) final TEM foil $\sim 8 \mu\text{m}$ in length and $\sim 100 \text{ nm}$ in thickness.

an ASM Eagle 60AP automatic wire bonder. An electrical flame off (EFO) process with a 48 mA current, 4500 V gap voltage and $290 \mu\text{s}$ discharge time produced a spherical copper ball under a shielding gas ($95\% \text{ N}_2 + 5\% \text{ H}_2$) introduced at a rate of 0.61 min^{-1} , to limit the oxidation of copper metal. Bonding was completed within 0.009 s using a combination of transverse ultrasonic vibration, a normal force (0.18 N) and heat ($175 \text{ }^\circ\text{C}$). Three ultrasonic power levels (UP1-28 DAC, UP2-36 DAC and UP3-45 DAC; here DAC is energy unit and is short for digital to analogue converter) were selected to study their effect on the interfacial structure and bonding strength. The ultrasonic amplitude of the capillary tip was measured with a laser interferometer, and they are 490.0 nm, 630.0 nm and 787.5 nm for the three power levels studied, respectively; the frequency remained at 138 kHz. All transmission electron microscopy (TEM) samples were prepared from the central regions of the Cu–Al interface by utilizing a FEI Nova 600 dual-beam focused ion beam (FIB) system, as shown in figure 1. TEM analysis was performed with a JEOL 2100F system at 200 kV. A nanoprobe beam (0.7 nm diameter) was employed for composition analysis with energy dispersive x-ray spectroscopy (EDX) in scanning (S)TEM mode. Fast Fourier transformation (FFT) of lattice images was calculated using ImageJ 1.42q [22] so as to identify Cu–Al IMCs. Shear tests were carried out with a DAGE 4000 micro-tester at a tool height of $3 \mu\text{m}$ and a tool movement speed of $4 \mu\text{m s}^{-1}$. The load that causes the fracture of the bonds is termed shear force. The shear strength was obtained as pressure, i.e. shear force per unit area. 20 bonds were measured for each condition.

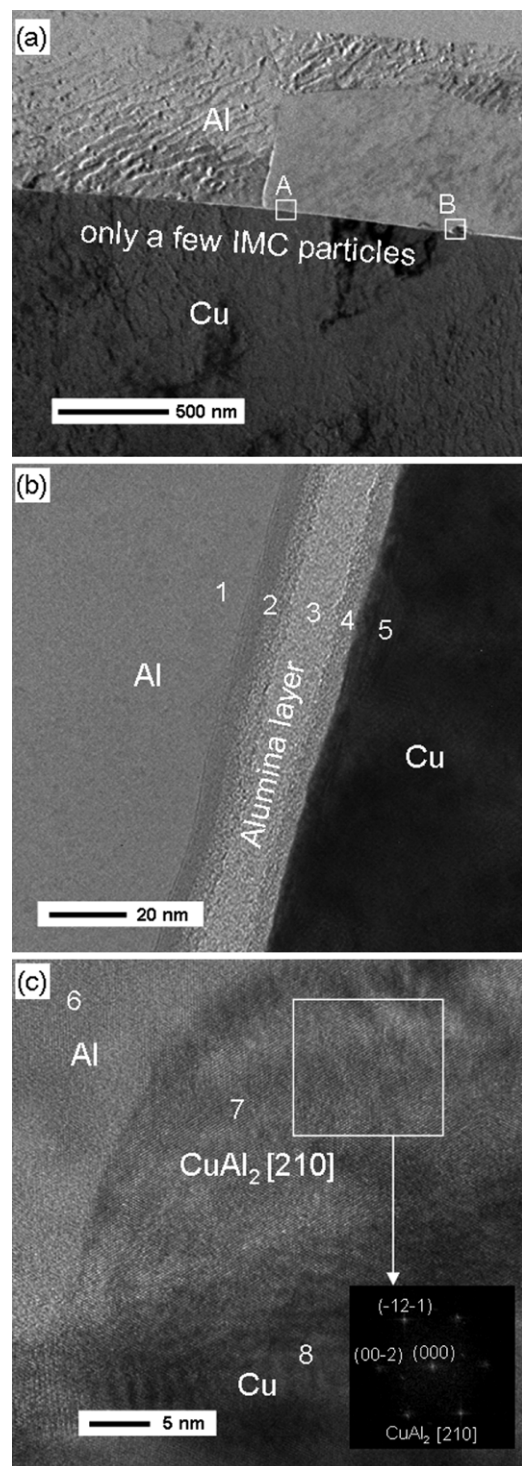


Figure 2. (a) TEM image of the Cu–Al interface for low power (Level UP1-28 DAC): only a few IMC particles were formed; (b) details of region A in (a) presenting an alumina layer between the copper ball and the aluminium pad; (c) lattice image and Fourier-reconstructed pattern of region B in (a) with $\text{CuAl}_2 [2 1 0]$.

3. Results and discussion

TEM studies showed that the Cu–Al interface consists of two distinct regions for all three levels of ultrasonic power applied (figures 2–4): (i) a uniform and compact alumina layer—a native oxide layer on the Al pad—in direct contact with Cu

Table 1. STEM-EDX results for regions 1–5 in figure 2(b) and 6–8 in figure 2(c). The precision of EDX measurement of O is approximately $\pm 10\%$, and Al and Cu are approximately $\pm 2\%$.

Regions	O K at%	Al K at%	Cu K at%
1	5	93	2
2	11	88	1
3	47	48	5
4	45	11	44
5	6	3	91
6	6	92	2
7	8	62	30
8	4	1	95

and (ii) regions containing IMCs. However, at a low ultrasonic power (Level UP1), the aluminium oxide layer occupies almost the entire interfacial region (figure 2(a)), as confirmed by a high magnification TEM image (figure 2(b)) and STEM-EDX analysis (table 1), which shows that the main constituents of the thin layer are aluminium and oxygen, indicating the existence of aluminium oxide layer that remains intact after bonding. The uniform layer of aluminium oxide acts as a barrier to interdiffusion of Cu and Al, so IMCs is unlikely to be formed in those regions. However, if the oxide layer is fragmented, formation of IMCs is possible. Only a few IMC particles (~ 15 nm thick) are formed during bonding with the low ultrasonic power (Level UP1). STEM-EDX results (table 1) show that the IMC is an aluminium-rich alloy. As a further confirmation, a lattice image (figure 2(c)) was collected in region A of figure 2(a) and FFT analysis is consistent with $[2\ 1\ 0]$ CuAl_2 ($I4/mcm$, $a = 6.067$ Å and $c = 4.877$ Å) [23].

As a higher ultrasonic power was applied, more IMCs were formed along the interface. The Cu–Al interface made at ultrasonic power 36 DAC (level UP2) is shown in figure 3(a). IMC particles occupy most interfacial regions. Figure 3(b) gives a lattice image taken in region A of figure 3(a). A Fourier-reconstructed pattern was obtained from the lattice image and was consistent with CuAl_2 $[0\ 0\ 1]$ abutting the Al pad. However, a few interfacial regions where IMCs are absent exist, and one of them is labelled B in figure 3(a). The details for region B in figure 3(a) were obtained with HRTEM and are presented in figure 3(c), confirming that some oxides remained uniform and intact after bonding. Nevertheless, ultrasonic power 45 DAC (Level UP3) resulted in an almost continuous layer of IMCs (figure 4). It is noteworthy that the IMCs have a conchoidal interface linked to Al and almost linear interface with Cu (figures 2(c), 3(a) and 4(a)), indicating the growth of those IMCs is dependent on the diffusion of Cu, i.e. Cu diffuses through IMCs to react with Al at the IMC/Al interface. In addition, the IMC thickness increased on increasing ultrasonic power, from ~ 15 nm at Level UP1 to ~ 30 nm at Level UP2 and to ~ 40 nm at Level UP3. The IMC phase remained the same— CuAl_2 , regardless of the levels of ultrasonic power applied in the study. Unlike the Au–Al bonds where voids were formed during the bonding process [14, 24], the Cu–Al bonds were void free.

It is confirmed that ultrasonic vibration partially disrupts the native aluminium oxide layer on the Al pad, which facilitates the formation of IMCs [12]. It is highlighted here

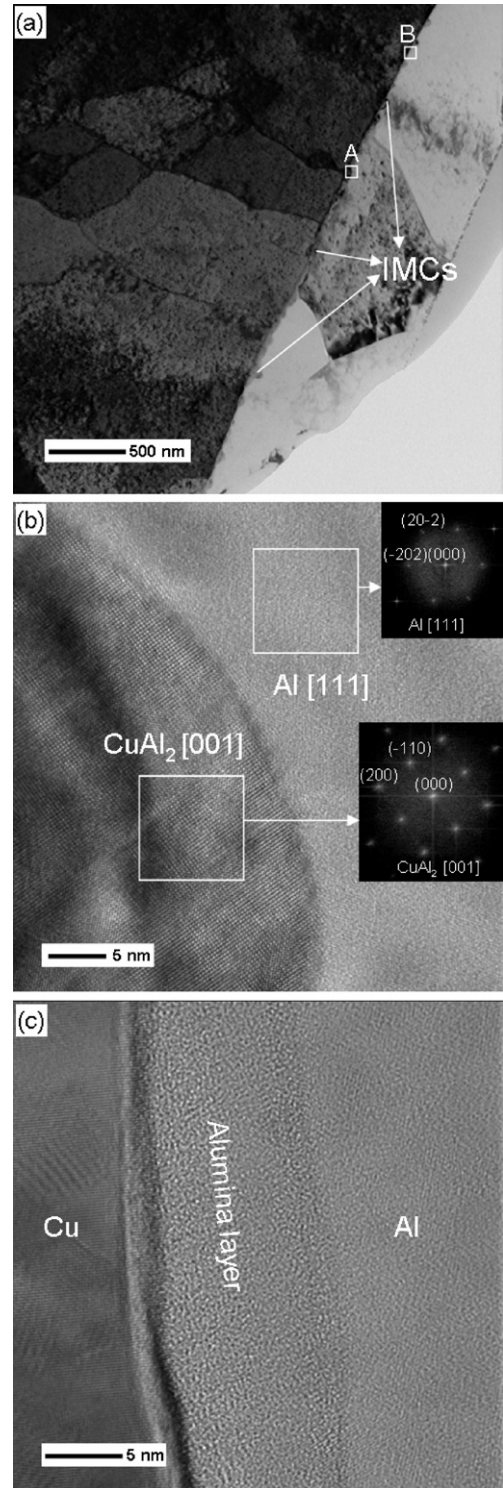


Figure 3. (a) TEM image of the Cu–Al interface for standard parameter setting (Level UP2-36 DAC): more IMC particles (~ 30 nm thick) at the interface; (b) lattice image and Fourier-reconstructed patterns of region A in (a) with CuAl_2 $[0\ 0\ 1]$ abutting Al $[1\ 1\ 1]$; (c) details of region B in (a) presenting uniform layer of alumina between Cu and Al.

that the magnitude of ultrasonic power determines the degree of fracture of the oxide layer, through which the formation of IMCs can initiate due to the direct contact of the metal surfaces to be bonded. Therefore, the quantity of IMCs formed during the bonding process is strongly dependent on

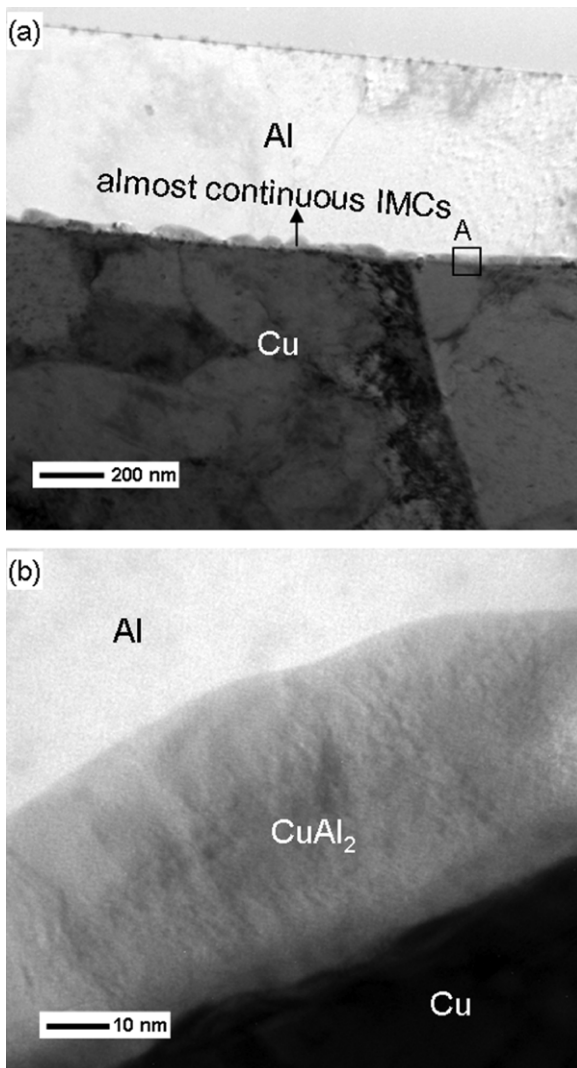


Figure 4. (a) TEM image of the Cu–Al interface for high ultrasonic power (Level UP3–45 DAC): almost continuous IMC layer (~ 40 nm) at the interface; (b) higher magnification of region A in (a) showing approximately 40 nm thick layer of CuAl_2 between Cu and Al.

the levels of ultrasonic power. For low ultrasonic power, the Cu–Al interface is occupied mostly by the native aluminium oxide layers, with only a few IMC particles being formed during bonding (figure 2). However, when high ultrasonic power is applied, aluminium oxide rupture becomes pervasive, so an almost continuous IMC layer is formed along the Cu/Al interface (figures 3 and 4), which provides a significant enhancement to the bonding strength, in agreement with shear tests which show that there was an obvious trend of increasing of shear force and shear strength with an increase in the ultrasonic power (figure 5). The areas of direct contact of alumina with Cu also contribute to bonding/adhesion, but their effect is less significant than the role played by the Cu–Al IMCs.

Although the initial formation of IMCs relies on fracture of the native oxide layer, the growth of IMCs is sustained by diffusion of Cu and Al through the IMC layer. The diffusivity of metals is influenced by the interfacial temperature and lattice structure of IMCs: the higher interfacial temperature and more

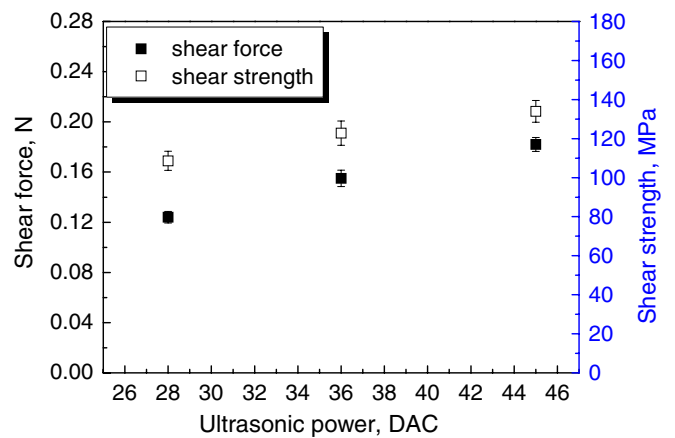


Figure 5. Higher ultrasonic power promotes IMCs of greater structured integrity that increase shear force and shear strength. The error bars are the standard deviation for 20 measured samples. (This figure is in colour only in the electronic version)

defects in the IMC lattice, the faster the diffusion process. A higher ultrasonic power not only breaks oxide over a larger area but also heats up the interface to a higher temperature and simultaneously creates more grain boundaries and dislocations [11], promoting the metal migration and, therefore, resulting in thicker IMCs, as observed ~ 15 nm thick IMCs for Level UP1, ~ 30 nm for Level UP2 and ~ 40 nm for Level UP3. Thus, IMCs occupy a larger area and have increased thickness, resulting in stronger bonds.

4. Conclusions

Formation of Cu–Al IMC CuAl_2 during thermosonic copper wire bonding correlates directly with ultrasonic power, and at high levels of the latter, the fragmentation of the native aluminium oxide becomes pervasive, resulting in continuous alloy interfaces and robust bonds. Formation of initial IMCs depends on oxide rupture by ultrasonic vibration, and the alloy growth is sustained by migration of Cu and Al through the initial IMC layers. A higher level of ultrasonic power not only breaks oxide over a larger total area but also creates more grain boundaries and dislocations to accelerate diffusivity, with IMCs occupying a larger area and having increased thickness, resulting in stronger bonds.

Acknowledgments

This research is financially supported by the UK Department for Innovation, Universities and Skills (DIUS) through the PMI2 project (Grant No RC 41). ASM Technology Singapore is acknowledged for providing wire-bond samples.

References

- [1] Mayer M, Paul O, Bolliger D and Baltes H 2000 *IEEE T. Compon. Pack. T.* **23** 393
- [2] Ho J R, Chen C C and Wang C H 2004 *Sensors Actuators A* **111** 188

- [3] Schneuwly A, Groning P, Schlapbach L and Muller G 1998 *J. Electron. Mater.* **27** 1254
- [4] Schwaller P, Groning P, Schneuwly A, Boschung P, Muller E, Blanc M and Schlapbach L 2000 *Ultrasonics* **38** 212
- [5] Groning P, Schwaller P, Schneuwly A and Schlapbach L 1999 *Surf. Interface Anal.* **28** 191
- [6] Lum I, Jung J P and Zhou Y 2005 *Metall. Mater. Trans. A* **36** 1279
- [7] Qi J, Hung N C, Li M and Liu D 2006 *Scr. Mater.* **54** 293
- [8] Zhou Y, Li X and Noolu N J 2005 *IEEE T. Compon. Pack. T.* **28** 810
- [9] Xu H, Liu C, Silberschmidt V V, Chen Z and Wei J 2010 *Microelectron. Int.* **27** 11
- [10] Xu H, Liu C, Silberschmidt V V, Chen Z and Wei J 2010 *J. Mater. Process. Tech.* **210** 1035
- [11] Li J, Han L, Duan J and Zhong J 2007 *Appl. Phys. Lett.* **90** 242902
- [12] Xu H, Liu C, Silberschmidt V V, Pramana S S, White T J and Chen Z 2009 *Scripta Mat.* **61** 165
- [13] Xu H, Liu C, Silberschmidt V V, Pramana S S, White T J, Chen Z, Sivakumar M and Acoff V L 2010 *J. Appl. Phys.* **108** 113517
- [14] Xu H, Liu C, Silberschmidt V V, Pramana S S, White T J, Chen Z, Sivakumar M and Acoff V L 2010 *J. Appl. Phys.* **108** 113517
- [15] Winchell V H and Berg H M 1978 *IEEE T. Compon. Hybrids Manuf. Tech.* **1** 211
- [16] Hulst A P and Lasance C 1978 *Weld. J.* **57** 19
- [17] Chen G K C 1972 *Int. Hybrid Microelectron. Symp. A* **5** 111
- [18] Mindlin R D 1949 *J. Appl. Mech.* **71** 259
- [19] Lum I, Mayer M and Zhou Y 2006 *J. Electron. Mater.* **35** 433
- [20] Lum I, Huang H, Chang B H, Mayer M, Du D and Zhou Y 2009 *J. Appl. Phys.* **105** 024905
- [21] Huang H, Pequegnat A, Chang B H, Mayer M, Du D and Zhou Y 2009 *J. Appl. Phys.* **106** 113514
- [22] Rasband W ImageJ Version 1.42q, National Institutes of Health, Bethesda, Maryland, USA 2009 <http://rsb.info.nih.gov/ij>
- [23] Meetsma A, de Boer J L and van Smaalen S 1989 *J. Solid State Chem.* **83** 370
- [24] Karpel A, Gur G, Atzmon Z and Kaplan W 2007 *J. Mater. Sci.* **42** 2334